

Supplementary Information – Traumatic brain injury on-a-chip: a microfluidic device for the compression of cortical spheroids

Mauricio Araiza Canizales^a, Alexander McGhee^b, Yang Wan^c, Jing Zhang^a, Emily Blick^d, Rafael D. González-Cruz^{efg}, Diane Hoffman-Kim^{efg}, Haneesh Kesari^c and Christian Franck^a.

^aDepartment of Mechanical Engineering, University of Wisconsin-Madison, Madison, US.

^bDepartment of Biomedical Engineering, University of Arizona, Tucson, US.

^cSchool of Engineering, Brown University, Providence, US.

^dDepartment of Biomedical Engineering, University of Wisconsin-Madison, Madison, US.

^eDepartment of Neuroscience, Brown University, Providence, US.

^fCarney Institute for Brain Science, Brown University, Providence, US.

^gInstitute for Biology, Engineering, and Medicine, Brown University, Providence, US.

Materials and methods

Inducing compressive injury in cortical spheroids

Table 1: Calibration data used for compression experiments of cortical spheroids.

Date	x1	y1	x2	y2	x3	y3	x4	y4	x5	y5	Target pressure (mbar)	Setpoint (mbar)	Max pressure (mbar)
5/17/2025	0	NA	100	NA	200	NA	300	NA	400	NA	NA	NA	NA
5/19/2025	0	NA	100	NA	200	NA	300	NA	400	NA	NA	NA	NA
6/9/2025	0	NA	100	NA	200	NA	300	NA	400	NA	NA	NA	NA
5/12/2025	0	NA	100	NA	200	NA	300	NA	400	NA	NA	NA	NA
5/15/2025	0	NA	100	NA	200	NA	300	NA	400	NA	NA	NA	NA
6/13/2025	0	NA	100	NA	200	NA	300	NA	400	NA	NA	NA	NA
3/12/2024	0	469.5	100	434.7	200	389.28	300	338.02	400	302.58	616.82	650	620
5/20/2025	0	434	100	400	200	356	300	314	400	278	574.15	600	596
6/11/2025	0	468.05	100	452	200	401.18	300	369.12	400	330.98	715.27	725	760.72
7/15/2025	0	481.84	300	443.26	600	409.1	900	386.36	1200	350.78	2846.68	2800	2869.6
7/16/2024	0	488.42	100	425	200	386.86	300	364.88	400	336.94	746.67	770	753
7/16/2025	0	460.5	300	436.72	600	387.32	900	309.3	1200	271.44	1887.15	1900	2098.38

Table 2: Cortical spheroid size and inferred strain and strain rate from compression experiments.

Date	Type	Timepoint	Major	Minor	Avg Size	Strain	Pulse width (s)	Strain rate (s ⁻¹)
5/17/2025	Control	0	272.955	265.006	269.0	0	NA	NA
	Control	0	233.124	233.124	233.1	0	NA	NA
	Control	0	237.773	228.544	233.2	0	NA	NA
	Control	0	241.128	233.128	237.1	0	NA	NA
	Control	0	289.609	268.336	279.0	0	NA	NA
	Control	0	267.06	229.134	248.1	0	NA	NA
5/19/2025	Control	0	246.624	244.463	245.5	0	NA	NA
	Control	0	295.927	287.364	291.6	0	NA	NA
	Control	0	233.704	225.121	229.4	0	NA	NA
	Control	0	268.767	255.868	262.3	0	NA	NA
	Control	0	246.576	246.576	246.6	0	NA	NA
	Control	0	257.336	253.028	255.2	0	NA	NA
6/9/2025	Control	0	270.069	260.139	265.1	0	NA	NA
	Control	0	238.223	238.223	238.2	0	NA	NA
	Control	0	269.365	265.087	267.2	0	NA	NA
	Control	0	256.624	250.2	253.4	0	NA	NA
	Control	0	292.688	241.783	267.2	0	NA	NA
	Control	0	272.872	268.592	270.7	0	NA	NA
5/13/2025	Control	24	282.615	264.98	273.8	0	NA	NA
	Control	24	284.813	276.735	280.8	0	NA	NA
	Control	24	313.539	289.23	301.4	0	NA	NA
	Control	24	305.374	297.338	301.4	0	NA	NA
	Control	24	304.67	275.941	290.3	0	NA	NA
	Control	24	320.138	293.647	306.9	0	NA	NA
5/15/2025	Control	24	332.772	311.973	322.4	0	NA	NA
	Control	24	273.457	256.547	265.0	0	NA	NA
	Control	24	316.61	314.278	315.4	0	NA	NA

Date	Type	Timepoint	Major	Minor	Avg Size	Strain	Pulse width (s)	Strain rate (s-1)
6/13/2025	Control	24	288.868	281.961	285.4	0	NA	NA
	Control	24	350.498	329.69	340.1	0	NA	NA
	Control	24	288.875	286.572	287.7	0	NA	NA
	Control	24	257.714	245.414	251.6	0	NA	NA
	Control	24	265.914	255.702	260.8	0	NA	NA
	Control	24	265.891	251.592	258.7	0	NA	NA
	Control	24	271.435	261.818	266.6	0	NA	NA
	Control	24	251.591	248.196	249.9	0	NA	NA
3/12/2024	Control	24	284.32	280.211	282.3	0	NA	NA
	Impact	0	294.781	275.111	284.9	0.28	0.138	2.03
	Impact	0	278.408	254.823	266.6	0.23	0.138	1.67
	Impact	0	269.223	269.223	269.2	0.24	0.138	1.74
	Impact	0	298.684	260.724	279.7	0.26	0.138	1.88
5/20/2025	IMO	0	289.56	269.268	279.4	NA	NA	NA
	IMO	0	279.07	273.195	276.1	NA	NA	NA
	Impact	0	290.437	273.69	282.1	0.3	0.06	5.00
	Impact	0	276.623	271.508	274.1	0.28	0.06	4.67
	Impact	0	270.718	266.388	268.6	0.26	0.06	4.33
	Impact	0	281.681	279.478	280.6	0.29	0.06	4.83
	IMO	0	267.831	259.831	263.8	NA	NA	NA
	IMO	0	270.718	266.388	268.6	NA	NA	NA
6/11/2025	Impact	0	274.899	274.899	274.9	0.27	0.1	2.70
	Impact	0	309.364	279.909	294.6	0.32	0.1	3.20
	Impact	0	318.683	312.212	315.4	0.36	0.1	3.60
	Impact	0	273.426	273.426	273.4	0.27	0.1	2.70
	IMO	0	284.232	260.527	272.4	NA	NA	NA
	IMO	0	294.957	271.292	283.1	NA	NA	NA
7/15/2025	Impact	24	256.52	218.26	237.4	0.25	0.12	2.08
	Impact	24	222.76	216.03	219.4	0.18	0.12	1.50

Date	Type	Timepoint	Major	Minor	Avg Size	Strain	Pulse width (s)	Strain rate (s-1)
7/16/2024	Impact	24	247.48	204.73	226.1	0.21	0.12	1.75
	Impact	24	259.52	228.78	244.2	0.27	0.12	2.25
	IMO	24	258.75	249.75	254.3	NA	NA	NA
	IMO	24	229.56	204.76	217.2	NA	NA	NA
	Impact	24	270.16	211.022	240.6	0.21	0.158	1.33
	Impact	24	285.91	274.768	280.3	0.32	0.158	2.03
	Impact	24	251.75	249.12	250.4	0.24	0.158	1.52
	Impact	24	251.73	245.206	248.5	0.24	0.158	1.52
	IMO	24	264.24	258.331	261.3	NA	NA	NA
7/17/2025	IMO	24	270.13	241.92	256.0	NA	NA	NA
	Impact	24	238.47	193.54	216.0	0.44	0.122	3.61
	Impact	24	184.58	176.28	180.4	0.44	0.122	3.61
	Impact	24	203.93	174.9	189.4	0.39	0.122	3.20
	Impact	24	220.51	186.65	203.6	0.46	0.122	3.77
	IMO	24	179.72	162.49	171.1	NA	NA	NA
	IMO	24	184.598	169.985	177.3	NA	NA	NA
					Average	0.29	0.12	2.77
					STDEV	0.07	0.03	1.15

Table 3: Summary of excluded cortical spheroids based on morphology, their baseline viability, as well as the image quality.

Date	Strain	Type	Timepoint	Sample number	Excluded?	Morphology	Baseline EthD-1	Image quality
5/17/2025	0	Control	0	1	TRUE	FALSE	TRUE	FALSE
5/17/2025	0	Control	0	2	TRUE	FALSE	TRUE	FALSE
5/17/2025	0	Control	0	4	TRUE	FALSE	TRUE	FALSE
5/17/2025	0	Control	0	5	TRUE	FALSE	TRUE	FALSE
5/17/2025	0	Control	0	6		FALSE	FALSE	FALSE
5/17/2025	0	Control	0	3		FALSE	FALSE	FALSE
5/19/2025	0	Control	0	1	TRUE	FALSE	TRUE	FALSE
5/19/2025	0	Control	0	2	TRUE	FALSE	TRUE	FALSE
5/19/2025	0	Control	0	3	TRUE	FALSE	FALSE	TRUE
5/19/2025	0	Control	0	4		FALSE	FALSE	FALSE
5/19/2025	0	Control	0	5	TRUE	FALSE	TRUE	FALSE
5/19/2025	0	Control	0	6	TRUE	TRUE	TRUE	FALSE
6/9/2025	0	Control	0	1		FALSE	FALSE	FALSE
6/9/2025	0	Control	0	2	TRUE	FALSE	TRUE	FALSE
6/9/2025	0	Control	0	3	TRUE	FALSE	TRUE	FALSE
6/9/2025	0	Control	0	4		FALSE	FALSE	FALSE
6/9/2025	0	Control	0	5		FALSE	FALSE	FALSE
6/9/2025	0	Control	0	6		FALSE	FALSE	FALSE
5/13/2025	0	Control	24	1	TRUE	FALSE	FALSE	TRUE
5/13/2025	0	Control	24	2	TRUE	FALSE	FALSE	TRUE
5/13/2025	0	Control	24	3	TRUE	FALSE	FALSE	TRUE
5/13/2025	0	Control	24	4	TRUE	FALSE	FALSE	TRUE
5/13/2025	0	Control	24	5	TRUE	FALSE	FALSE	TRUE
5/13/2025	0	Control	24	6	TRUE	FALSE	FALSE	TRUE
5/15/2025	0	Control	24	1	TRUE	FALSE	FALSE	TRUE
5/15/2025	0	Control	24	2	TRUE	TRUE	TRUE	FALSE
5/15/2025	0	Control	24	3		FALSE	FALSE	FALSE
5/15/2025	0	Control	24	4	TRUE	FALSE	TRUE	FALSE
5/15/2025	0	Control	24	5	TRUE	FALSE	FALSE	TRUE

5/15/2025	0	Control	24	6	TRUE	FALSE	TRUE	FALSE
6/13/2025	0	Control	24	1		FALSE	FALSE	FALSE
6/13/2025	0	Control	24	2	TRUE	TRUE	TRUE	FALSE
6/13/2025	0	Control	24	3		FALSE	FALSE	FALSE
6/13/2025	0	Control	24	4		FALSE	FALSE	FALSE
6/13/2025	0	Control	24	5	TRUE	FALSE	TRUE	FALSE
6/13/2025	0	Control	24	6	TRUE	FALSE	TRUE	FALSE
3/12/2024	25	Impact	0	1		FALSE	FALSE	FALSE
3/12/2024	25	Impact	0	2		FALSE	FALSE	FALSE
3/12/2024	25	Impact	0	3		FALSE	FALSE	FALSE
3/12/2024	25	Impact	0	4	TRUE	FALSE	TRUE	FALSE
3/12/2024	25	IMO	0	1		FALSE	FALSE	FALSE
3/12/2024	25	IMO	0	2		FALSE	FALSE	FALSE
5/20/2025	25	Impact	0	1	TRUE	FALSE	TRUE	FALSE
5/20/2025	25	Impact	0	2	TRUE	FALSE	TRUE	FALSE
5/20/2025	25	Impact	0	3	TRUE	FALSE	TRUE	FALSE
5/20/2025	25	Impact	0	4	TRUE	FALSE	TRUE	TRUE
5/20/2025	25	IMO	0	1	TRUE	FALSE	TRUE	FALSE
5/20/2025	25	IMO	0	2	TRUE	FALSE	TRUE	FALSE
6/11/2025	25	Impact	0	1	TRUE	FALSE	TRUE	FALSE
6/11/2025	25	Impact	0	2		FALSE	FALSE	FALSE
6/11/2025	25	Impact	0	3		FALSE	FALSE	FALSE
6/11/2025	25	Impact	0	4		FALSE	FALSE	FALSE
6/11/2025	25	IMO	0	1		FALSE	FALSE	FALSE
6/11/2025	25	IMO	0	2		FALSE	FALSE	FALSE
7/15/2025	25	Impact	24	1		FALSE	FALSE	FALSE
7/15/2025	25	Impact	24	2	TRUE	TRUE	TRUE	FALSE
7/15/2025	25	Impact	24	3	TRUE	TRUE	TRUE	FALSE
7/15/2025	25	Impact	24	4	TRUE	TRUE	TRUE	FALSE
7/15/2025	25	IMO	24	1		FALSE	FALSE	FALSE
7/15/2025	25	IMO	24	2		FALSE	FALSE	FALSE
7/16/2024	25	Impact	24	1	TRUE	TRUE	FALSE	TRUE

7/16/2024	25	Impact	24	2	TRUE	FALSE	TRUE	FALSE
7/16/2024	25	Impact	24	3	TRUE	FALSE	FALSE	TRUE
7/16/2024	25	Impact	24	4	TRUE	FALSE	FALSE	TRUE
7/16/2024	25	IMO	24	1	TRUE	FALSE	FALSE	TRUE
7/16/2024	25	IMO	24	2	TRUE	TRUE	FALSE	TRUE
7/17/2025	25	Impact	24	1		FALSE	FALSE	FALSE
7/17/2025	25	Impact	24	2		FALSE	FALSE	FALSE
7/17/2025	25	Impact	24	3		FALSE	FALSE	FALSE
7/17/2025	25	Impact	24	4		FALSE	FALSE	FALSE
7/17/2025	25	IMO	24	1		FALSE	FALSE	FALSE
7/17/2025	25	IMO	24	2		FALSE	FALSE	FALSE

Excluded spheroids	42
Used spheroids	30
Morphology	8
Baseline EthD-1	28
Image quality	15

Fixation and immunohistochemistry of cortical spheroids

Table 4: List of antibodies used in the primary antibody solution, as well as their respective concentration and volume used for compression experiments of cortical spheroids.

Antibody	Species	Catalog #	Lot #	Concentration	Volume (μL)
GFAP	Chicken	PA1-10004	YF3963761	1:200	7.5
β -III	Mouse	MA1-19187	ZC4239062	1:200	7.5
NFL	Rabbit	12998-1-AP	00110327	1:200	7.5
Blocking solution	-	-	-	-	1477.5

Table 5: List of antibodies used in the secondary antibody solution, as well as their respective concentration, volume and probe wavelength used for compression experiments of cortical spheroids.

Antibody	Species	Wavelength	Catalog #	Lot #	Concentration	Volume (μL)
GFAP	Goat	555	A32932	YB363611	1:200	7.5
β -III	Goat	647	A32728	WE322197	1:200	7.5
NFL	Goat	488	A32731	WI329965	1:200	7.5
Blocking solution	-	-	-	-	-	1477.5

Quantifying protein recovery

Quantification of protein recovery across the microfluidic device was performed using a standard Rat TNF- α ELISA kit (LEGEND MAX Rat TNF- α ELISA kit, BioLegend, San Diego, CA, USA). Briefly, 2 sets of 250 μL stock solutions of decreasing TNF- α concentrations ranging from 500 to 7.8 $\mu\text{g}/\text{mL}$ were aliquoted into 2 mL tubes and stored in ice. Additionally, 2 more aliquots of the same volume containing a buffer solution were used as a 0 $\mu\text{g}/\text{mL}$ baseline. A 1 mL syringe was loaded with buffer solution and loaded into a syringe pump (Fusion 200, Chemyx, Stafford, TX, USA). The volume of solution was injected into the microfluidic device through the media inlet port at a constant rate of 50 $\mu\text{L}/\text{min}$ (3 mL/hr) after which the recovered volume of solution was collected at the cell culture media reservoir. The recovered solution was stored in an empty 2 mL tube and placed once again in ice. Prior to loading the subsequent solutions, the microfluidic chip was rinsed with 1 mL of distilled water which was injected at a rate of 200 $\mu\text{L}/\text{min}$ (12 mL/hr) and dried by flushing air. The process was repeated for all other solutions after which an ELISA was performed on the recovered solution according to the manufacturer's instructions. A set of aliquots remained in ice for the duration of the experiment and served for calibration and as the known inlet concentration.

Figures

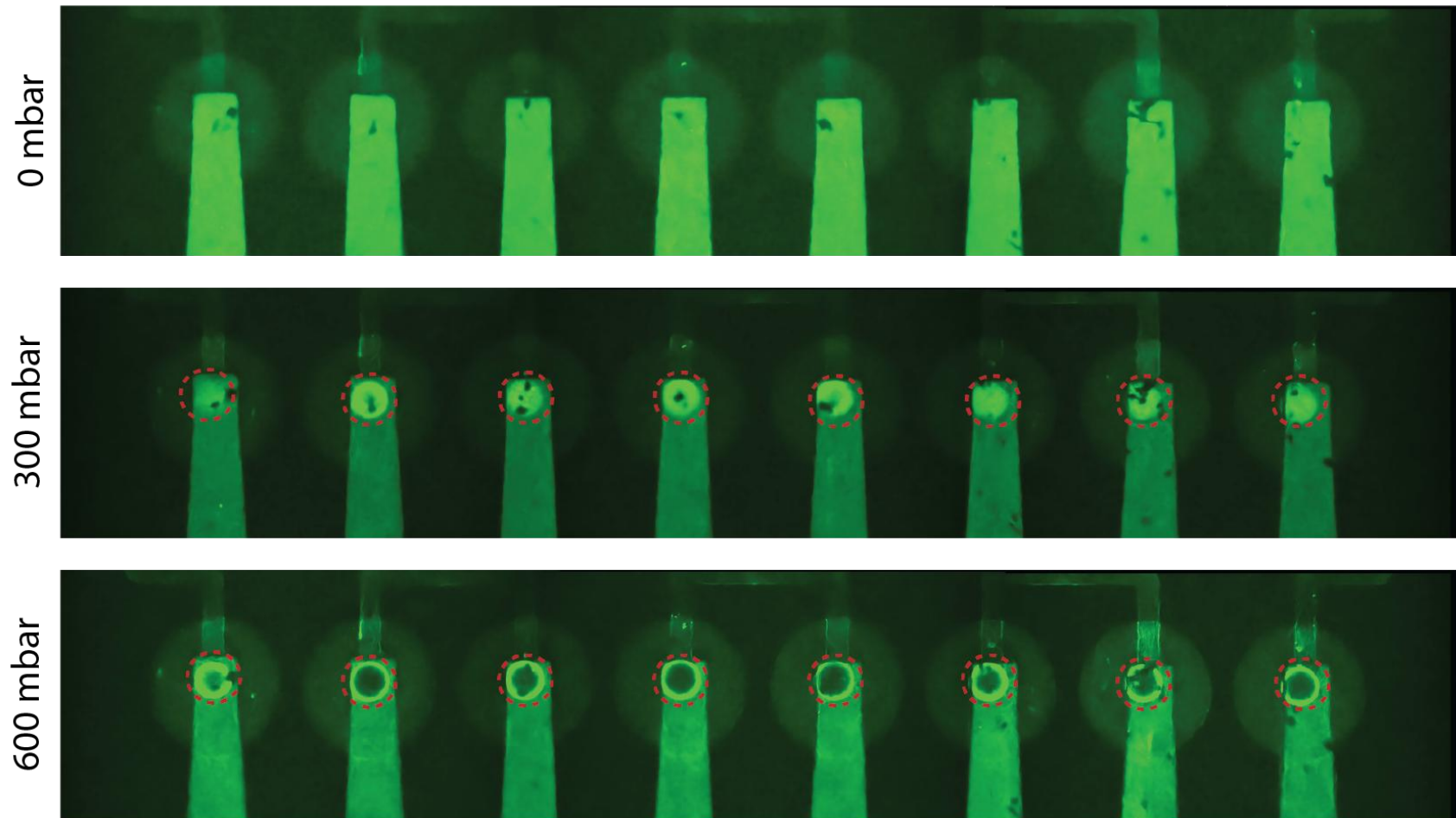


Figure 1: Quasi-static response of multiple PDMS pillars under different pressures. Images were taken $250\ \mu\text{m}$ from the bottom of the cortical spheroid trap. As the pressure increases all the PDMS pillars get in focus at the same time, showing that their displacement is similar across all channels.

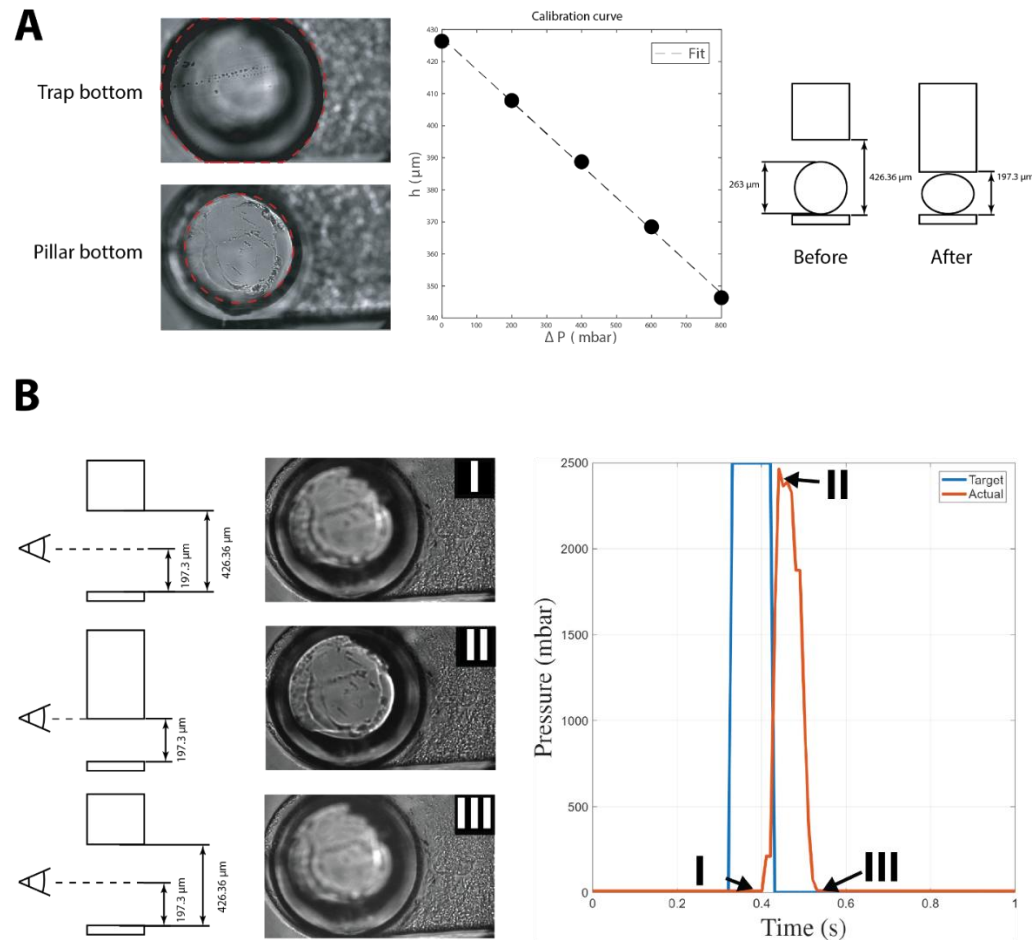


Figure 2: Transient response of PDMS pillars under a pressure impulse response. (A) Calibration curve showing the bottom of the spheroid trap, as well as the bottom of the PDMS pillar. Schematic showing the average height of a cortical spheroid of 263 μm in diameter compressed to 25% strain as indicated by the location of the PDMS pillar. (B) Snapshots of a high-speed video recorded at 200 frames per second of the pillar displacement. I) PDMS pillar out of focus moments before the pressure spike. II) PDMS pillar in focus at the required height to achieve 25% strain and at the maximum pressure. III) PDMS pillar returning to its original position after the pressure impulse ends.

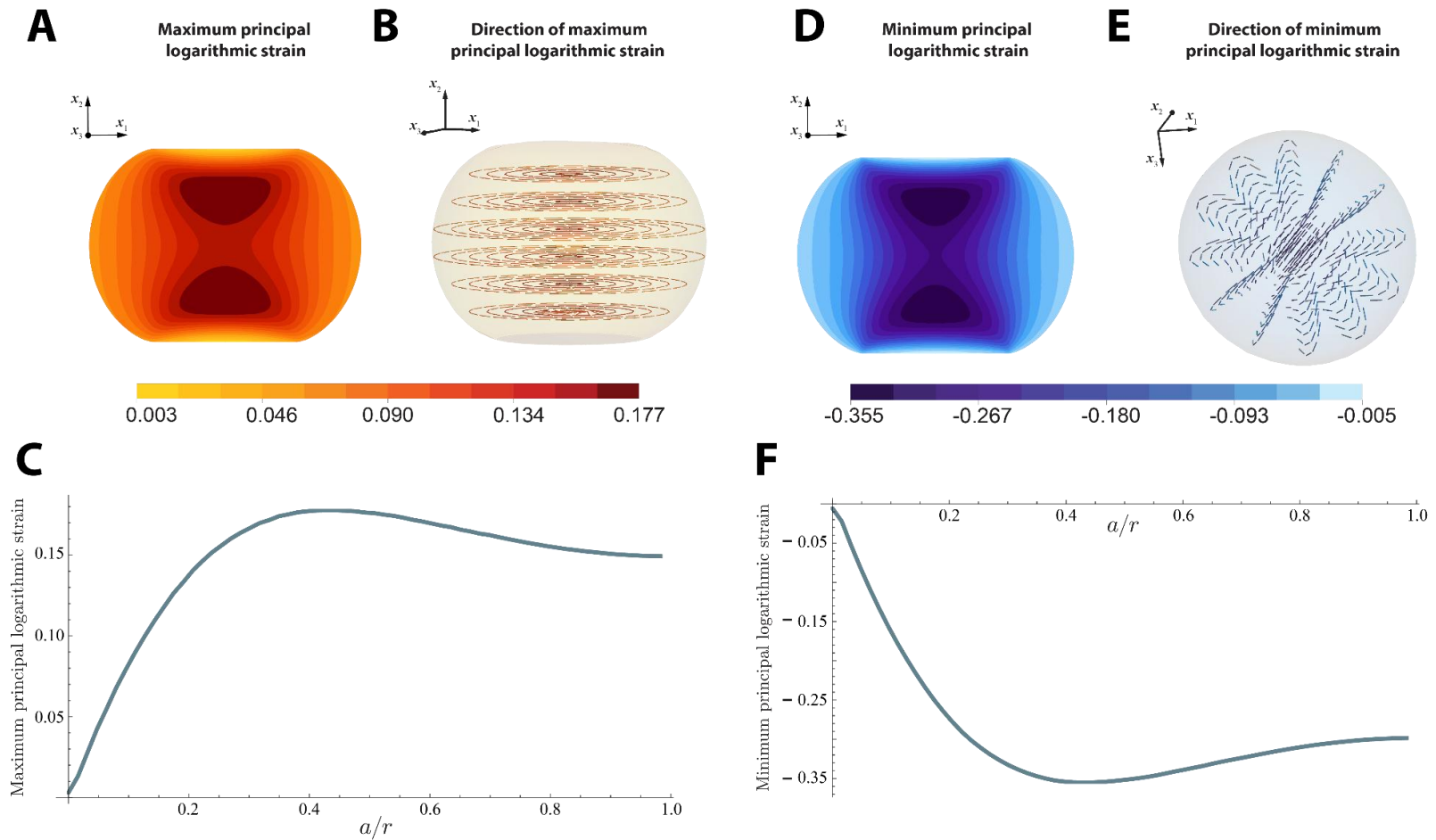


Figure 3: Finite element model results for the compression of an idealized 250 μm diameter cortical organoid at 25% prescribed global compressive nominal strain. (A) and (D) Contour plots showing the maximum and minimal principal logarithmic strain, respectively. (B) and (E) Corresponding directions of the maximum and minimum principal logarithmic strains. (C) and (F) Plots of the maximum and minimum logarithmic strains as a function of the ratio of the distance from the bottom of the sphere to its center, a , to the radius.

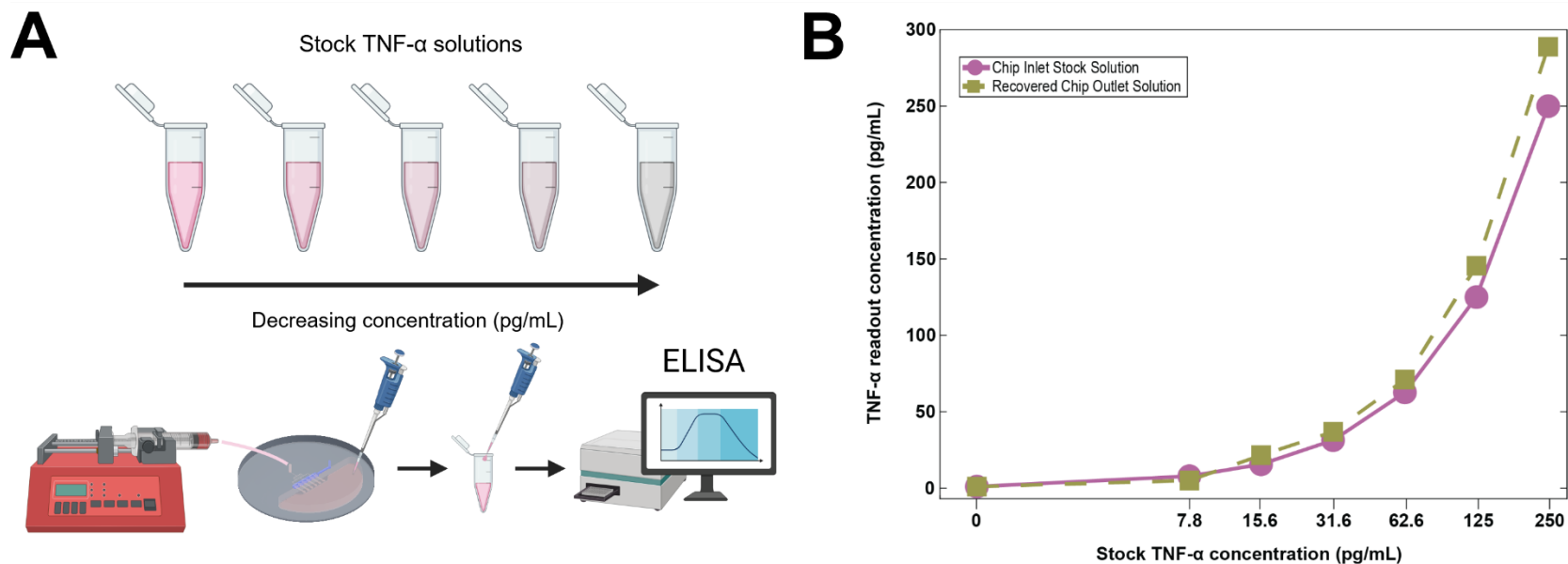


Figure 4: Experimental workflow and results for the recovery analysis of TNF- α after being injected into the microfluidic chip simulating the analysis of 0⁺ timepoints. (A) Stock solutions of decreasing concentration of TNF- α were aliquoted and subsequently loaded into a syringe pump and injected at a controlled rate (3 mL/hr) in the chip's media inlet. The recovered media was then analyzed using an ELISA plate reader. (B) TNF- α readout concentrations for the chip inlet stock solution and the recovered outlet solution. X-axis is logarithmic scale.